5. Production of high P_T jets

5.1 Introduction

5.2 Reminder: the structure of QCD, calculation of matrix elements

5.3 Jet production at hadron colliders

5.4 Impact on parton distribution functions

5.5 Direct photon production

5.6 Measurements of α_s

5.1 Introduction

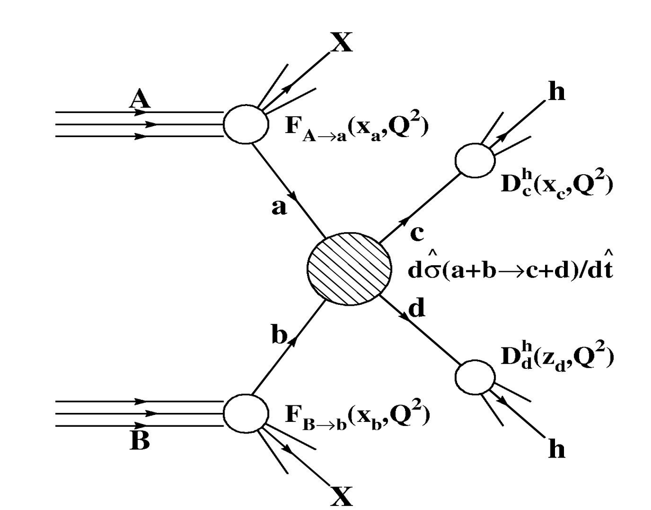

Leading order

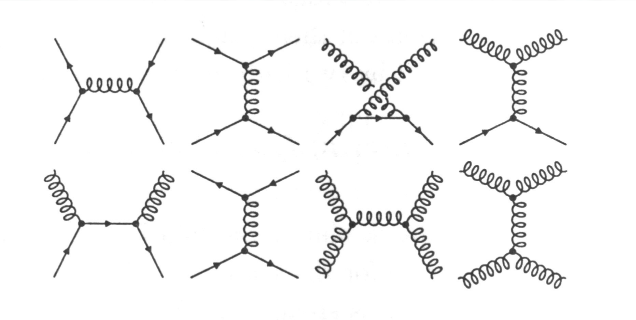

…some NLO contributions

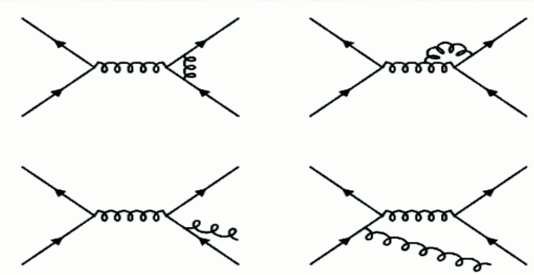

- Hard scattering processes at hadron colliders are dominated by jet production
- QCD process, originating from qq, qg and gg scattering
- Cross sections can be calculated in QCD (perturbation theory)

Comparison between experimental data and theoretical predictions constitutes an important test of the theory.

Deviations?
→ Problem in the experiment ?
Problem in the theory (QCD) ?
New Physics, e.g. quark substructure ?

- Large cross sections….
- Fast rising with √s

Leading order

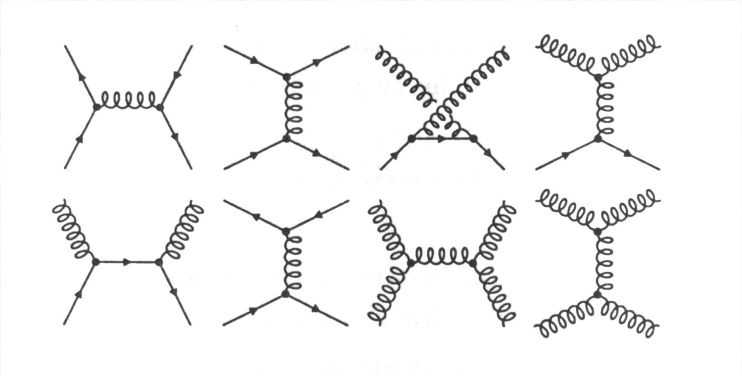

…some NLO contributions

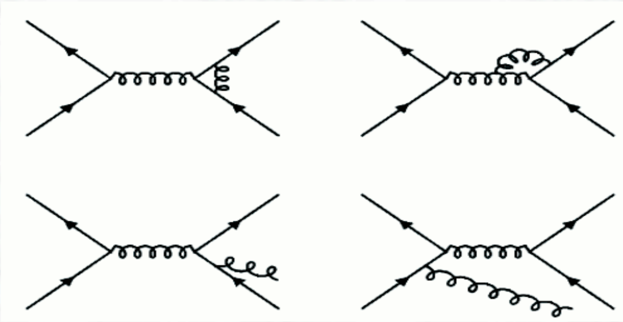

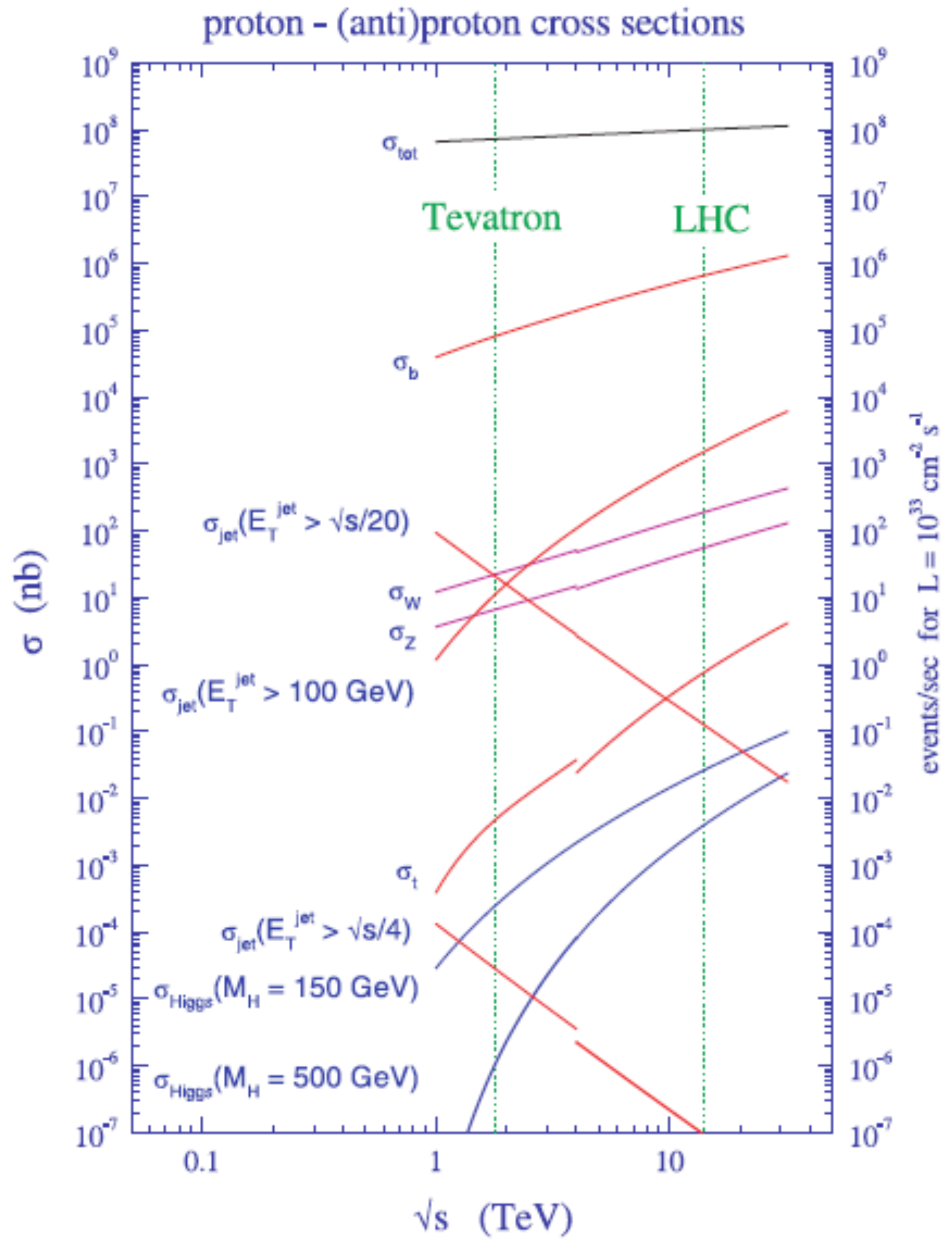

Cross sections for important hard scattering Standard Model processes at the Tevatron and the LHC colliders

Jets from QCD production: Tevatron vs LHC

- Rapidly probe perturbative QCD in a new energy regime (at a scale above the Tevatron, large cross sections)

- Experimental challenge: understanding of the detector
  - main focus on jet energy scale
  - resolution

- Theory challenge:
  - improved calculations…
    (renormalization and factorization scale uncertainties)
  - pdf uncertainties

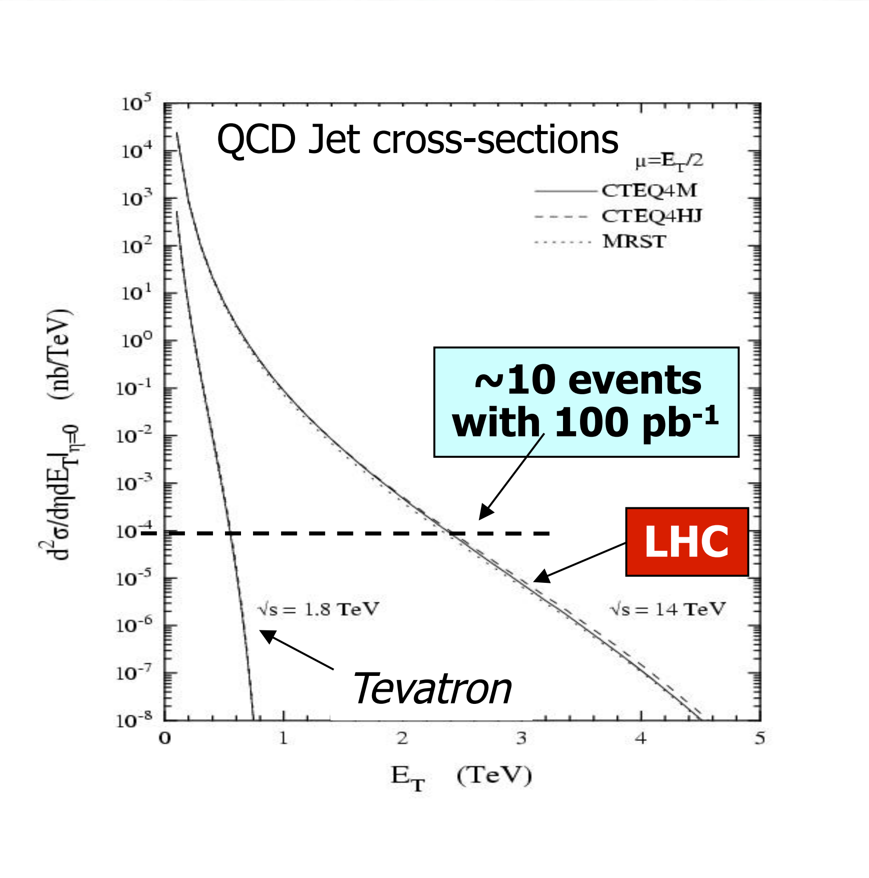

5.2 Reminder: structure of QCD, matrix element calculation

Theory	Interaction	charge	Gauge boson
QED	electromagnetic	electric charge	Photon
QCD	strong	colour charge	Gluons

Coupling constants

$g_e = \sqrt{4\pi\alpha}$ QED

$g_s = \sqrt{4\pi\alpha_s}$ QCD

Gluon Colour states

$c = \begin{pmatrix} 1 \\ 0 \\ 0 \end{pmatrix}$ red

$c = \begin{pmatrix} 0 \\ 1 \\ 0 \end{pmatrix}$ blue

$c = \begin{pmatrix} 0 \\ 0 \\ 1 \end{pmatrix}$ green

SU3:

Color Octet

$$|1\rangle = (r\bar{b} + b\bar{r})/\sqrt{2}$$
$$|2\rangle = -i(r\bar{b} - b\bar{r})/\sqrt{2}$$
$$|3\rangle = (r\bar{r} - b\bar{b})/\sqrt{2}$$
$$|4\rangle = (r\bar{g} + g\bar{r})/\sqrt{2}$$
$$|5\rangle = -i(r\bar{g} - g\bar{r})/\sqrt{2}$$
$$|6\rangle = (b\bar{g} + g\bar{b})/\sqrt{2}$$
$$|7\rangle = -i(b\bar{g} - g\bar{b})/\sqrt{2}$$
$$|8\rangle = (r\bar{r} + b\bar{b} + 2g\bar{g})/\sqrt{6}$$

Color Singlet

$$|9\rangle = -i(r\bar{r} + b\bar{b} + g\bar{g})/\sqrt{3}$$

Color Singlet gluons do not exist. Since the gluons have m=0, this would give a strong gravity force.

Quark and gluon states:

a quark is
characterized by
- momentum p
- spin state s
- color state c

$$u^{(s)}(p)c$$

a gluon is
characterized by
- momentum p
- polarisation ε
- color state a^α

$$\epsilon_\mu(p)a^\alpha$$

Color states of the gluon

$$a^1 = \begin{pmatrix} 1 \\ 0 \\ 0 \\ 0 \\ 0 \\ 0 \\ 0 \\ 0 \end{pmatrix}, \quad a^2 = \begin{pmatrix} 0 \\ 1 \\ 0 \\ 0 \\ 0 \\ 0 \\ 0 \\ 0 \end{pmatrix}, \ \ldots$$

Gluons carry color charge, therefore they can couple to each other.
This is not possible for photons.

The Gell-Mann λ-matrices are the generators of SU3, equivalent to the Pauli matrices for SU2.

$$\lambda^1 = \begin{pmatrix} 0 & 1 & 0 \\ 1 & 0 & 0 \\ 0 & 0 & 0 \end{pmatrix} \quad \lambda^2 = \begin{pmatrix} 0 & -i & 0 \\ i & 0 & 0 \\ 0 & 0 & 0 \end{pmatrix} \quad \lambda^3 = \begin{pmatrix} 1 & 0 & 0 \\ 0 & -1 & 0 \\ 0 & 0 & 0 \end{pmatrix} \quad \lambda^4 = \begin{pmatrix} 0 & 0 & 1 \\ 0 & 0 & 0 \\ 1 & 0 & 0 \end{pmatrix}$$

$$\lambda^5 = \begin{pmatrix} 0 & 0 & -i \\ 0 & 0 & 0 \\ i & 0 & 0 \end{pmatrix} \quad \lambda^6 = \begin{pmatrix} 0 & 0 & 0 \\ 0 & 0 & 1 \\ 0 & 1 & 0 \end{pmatrix} \quad \lambda^7 = \begin{pmatrix} 0 & 0 & 0 \\ 0 & 0 & -i \\ 0 & i & 0 \end{pmatrix} \quad \lambda^8 = \frac{1}{\sqrt{3}} \begin{pmatrix} 1 & 0 & 0 \\ 0 & 1 & 0 \\ 0 & 0 & -2 \end{pmatrix}$$

The commutators of the λ-matrices define the structure constants of SU3.

$$[\lambda^\alpha,\ \lambda^\beta] = 2if^{\alpha\beta\gamma}\lambda^\gamma$$

with $f^{\beta\alpha\gamma} = f^{\alpha\gamma\beta} = -f^{\alpha\beta\gamma}$

completely antisymmetric

There are 8x8x8=512 structure constants.
Most are zero, except for the following and their antisymmetric permutations.

$$f^{123} = 1$$

$$f^{147} = f^{246} = f^{257} = f^{345} = f^{516} = f^{637} = \frac{1}{2}$$

$$f^{458} = f^{678} = \sqrt{\frac{3}{2}}$$

Feynman rules for QCD:

1. External Lines

Quark	incoming	$u^{(s)}(p)c$
	outgoing	$\bar{u}^{(s)}(p)c^{+}$
Antiquark	incoming	$\bar{v}^{(s)}(p)c^{+}$
	outgoing	$v^{(s)}(p)c$
Gluon	incoming	$\epsilon_{\mu}(p)a^{\alpha}$
	outgoing	$\epsilon^{*}_{\mu}(p)\,(a^{\alpha})^{*}$

2. Propagators

$q, \bar{q}$ $\qquad \dfrac{i(\gamma^{\mu} q_{\mu} + mc)}{q^2 - m^2 c^2}$

g $\qquad \dfrac{-i g_{\mu\nu} \delta^{\alpha\beta}}{q^2}$

3. Vertices

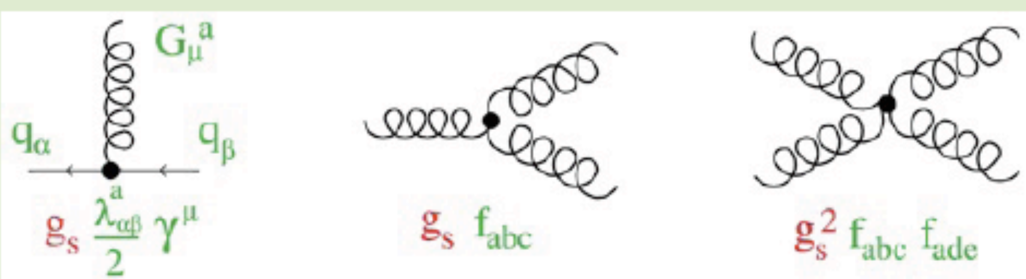

4. Internal Loop Diagrams

More complicated than in QED.
Not treated here.

5. δ-function for momentum conservation

Example: invariant amplitude for u dbar → u dbar scattering

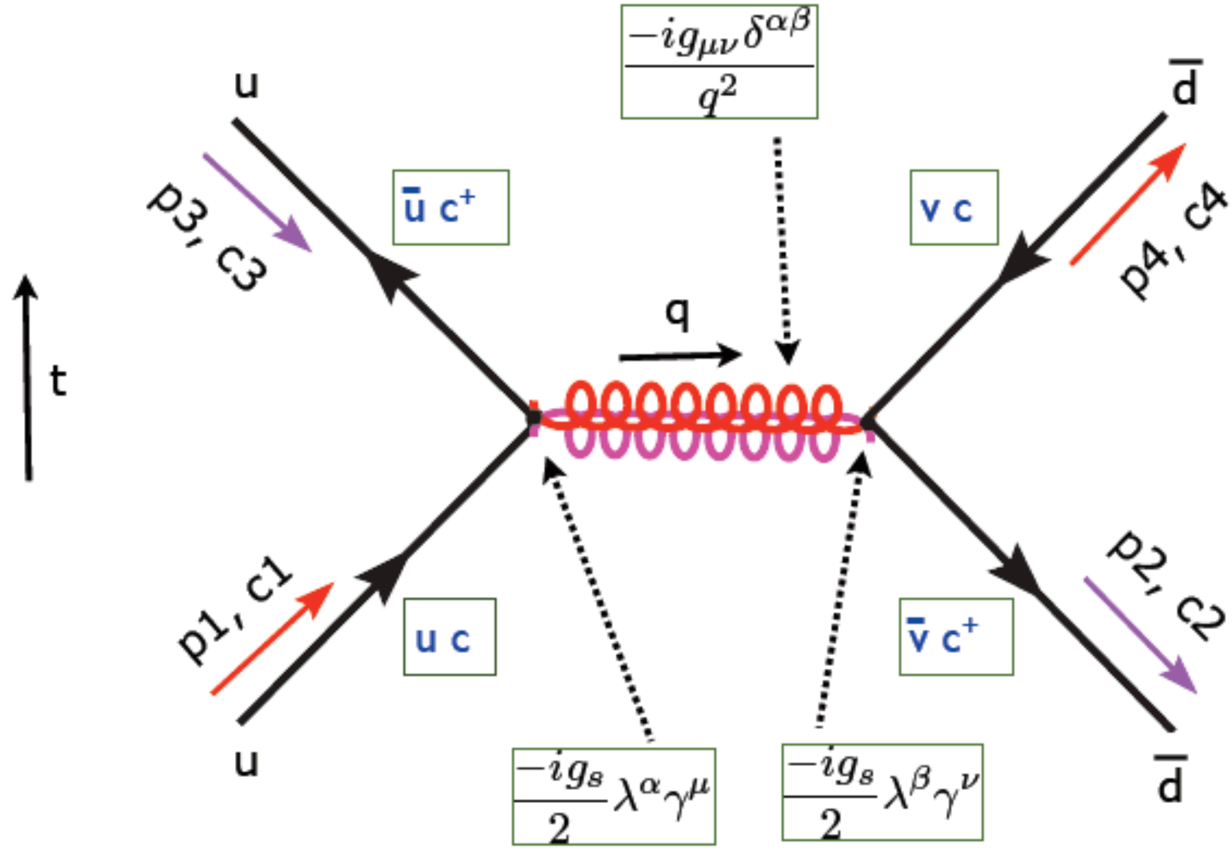

Like in QED also in QCD the charge is conserved.

Thus diagrams have continuous flow of color.

Matrix elements are like in QED, but they contain a color factor.

$$-i\mathcal{M} = \bar{u}(3)c_3^+\left[-i\frac{g_s}{2}\lambda^\alpha\gamma^\mu\right]u(1)c_1\frac{-ig_{\mu\nu}\delta^{\alpha\beta}}{q^2}\bar{v}(2)c_2^+\left[-i\frac{g_s}{2}\lambda^\beta\gamma^\nu\right]v(4)c_4$$

$$\mathcal{M} = \frac{-g_s^2}{4q^2}\left[\bar{u}(3)\gamma^\mu u(1)\right]\left[\bar{v}(2)\gamma_\mu v(4)\right]\left[c_3^+\lambda^\alpha c_1\right]\left[c_2^+\lambda^\alpha c_4\right]$$

Example (ii): u ubar → gg

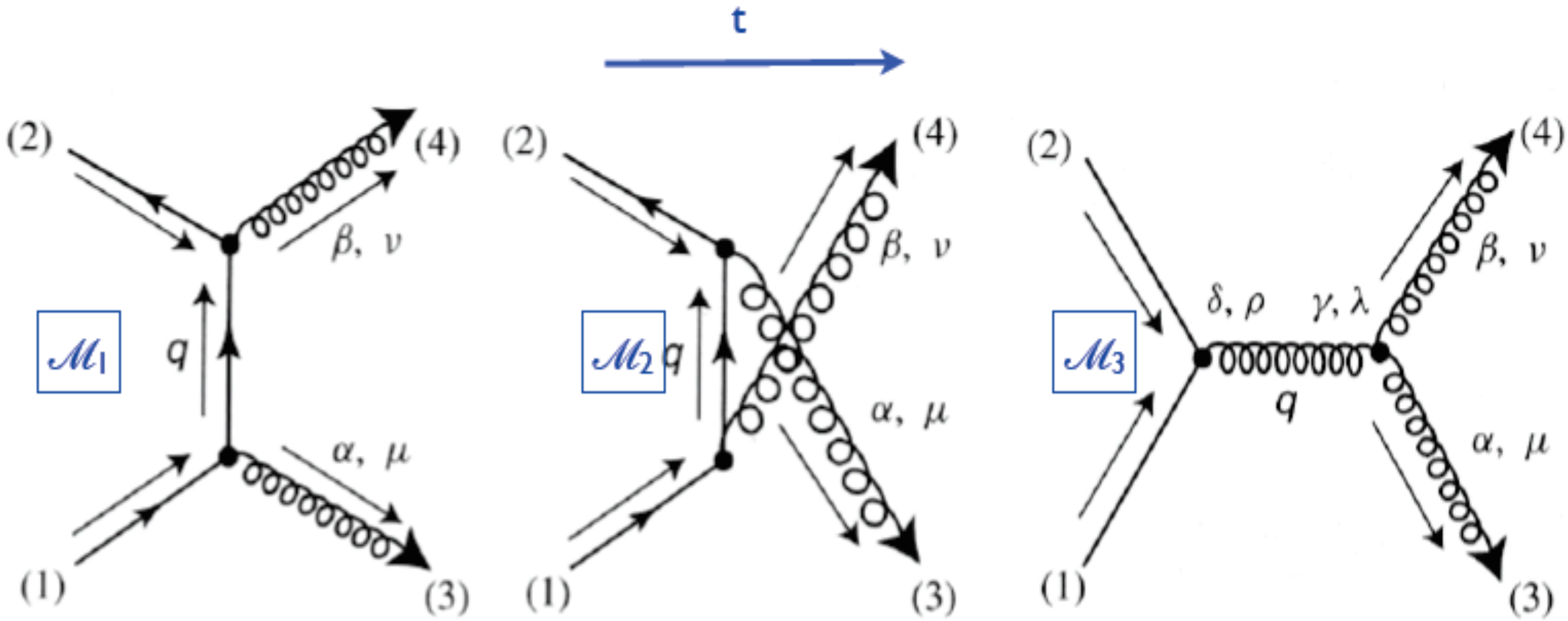

$$\mathscr{M}_1 = i\bar{v}(2)c_2^\dagger\left[-i\frac{g_s}{2}\lambda^\beta\gamma^\nu\right][\epsilon^*_{4\nu}a_4^{\beta *}]\left[\frac{i(\not{q}+mc)}{q^2-m^2c^2}\right] \times\left[-i\frac{g_s}{2}\lambda^\alpha\gamma^\mu\right][\epsilon^*_{3\mu}a_3^{\alpha *}]u(1)c_1$$

$$\mathscr{M}_3 = i\bar{v}(2)c_2^\dagger\left[-i\frac{g_s}{2}\lambda^\delta\gamma_\sigma\right]u(1)c_1\left[-i\frac{g^{\sigma\lambda}\delta^{\delta\gamma}}{q^2}\right]\{-g_s f^{\alpha\beta\gamma}[g_{\mu\nu}(-p_3+p_4)_\lambda + g_{\nu\lambda}(-p_4-q)_\mu + g_{\lambda\mu}(q+p_3)_\nu]\}[\epsilon_3^\mu a_3^\alpha][\epsilon_4^\nu a_4^\beta]$$

$$\mathscr{M}_2 = \frac{-g_s^2}{8}\frac{1}{p_1\cdot p_4}\left\{\bar{v}(2)[\not{\epsilon}_3(\not{p}_1-\not{p}_4+mc)\not{\epsilon}_4]u(1)\right\}a_3^\alpha a_4^\beta(c_2^\dagger\lambda^\alpha\lambda^\beta c_1)$$

colour flow in hard processes:

One Feynman graph can correspond to several possible colour flows, e.g. for $qg \to qg$:

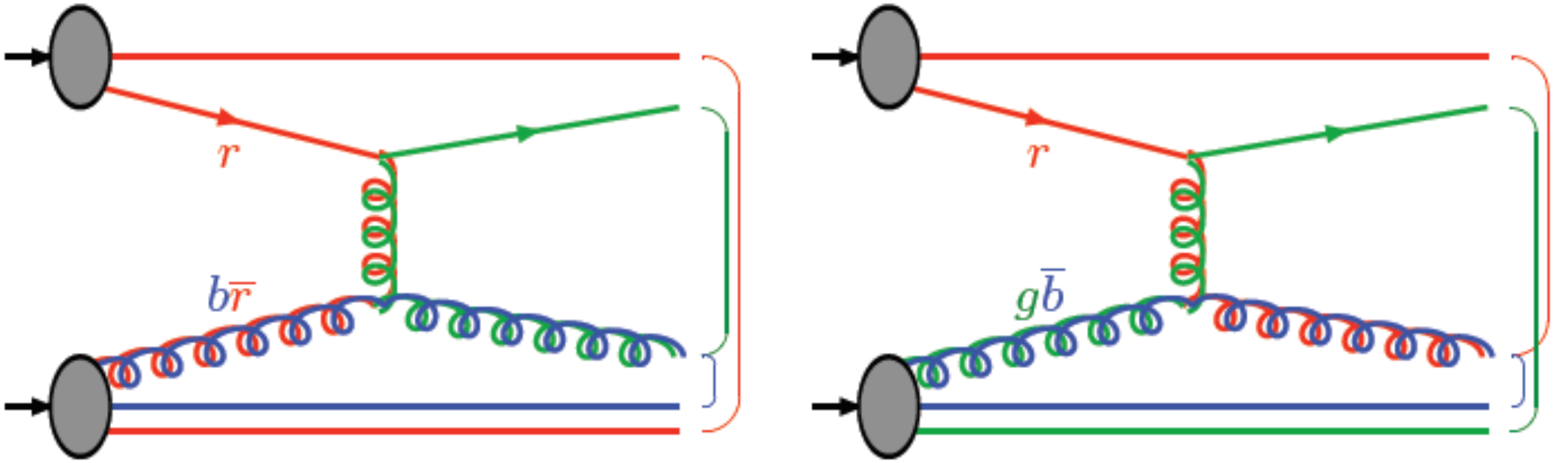

while other $qg \to qg$ graphs only admit one colour flow:

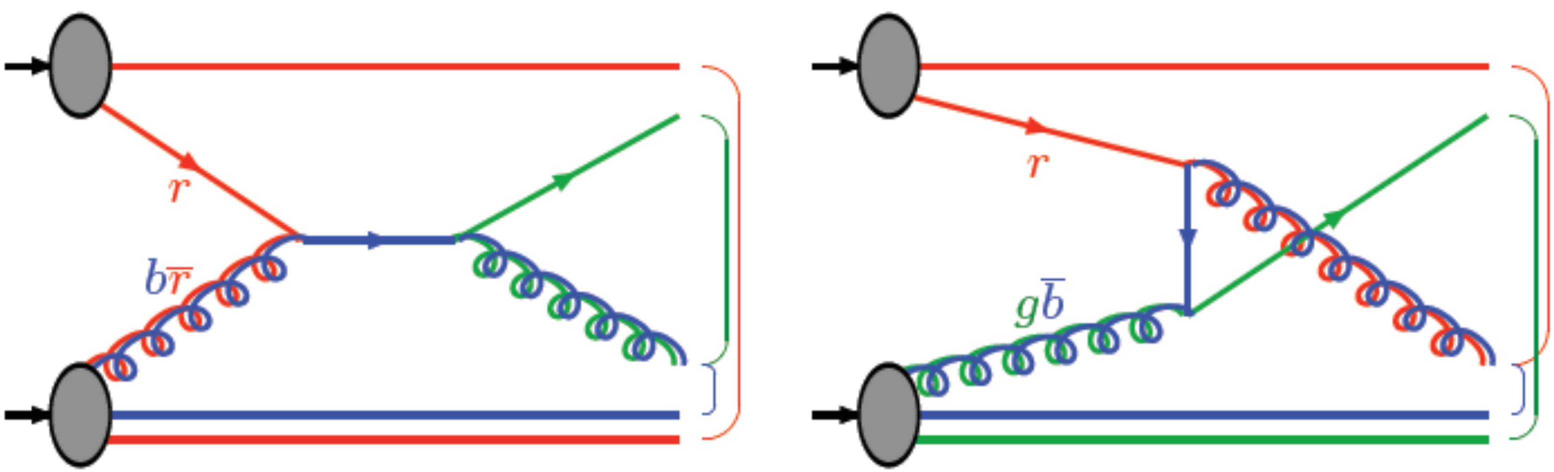

Quarks and gluon loops, running of α_s:

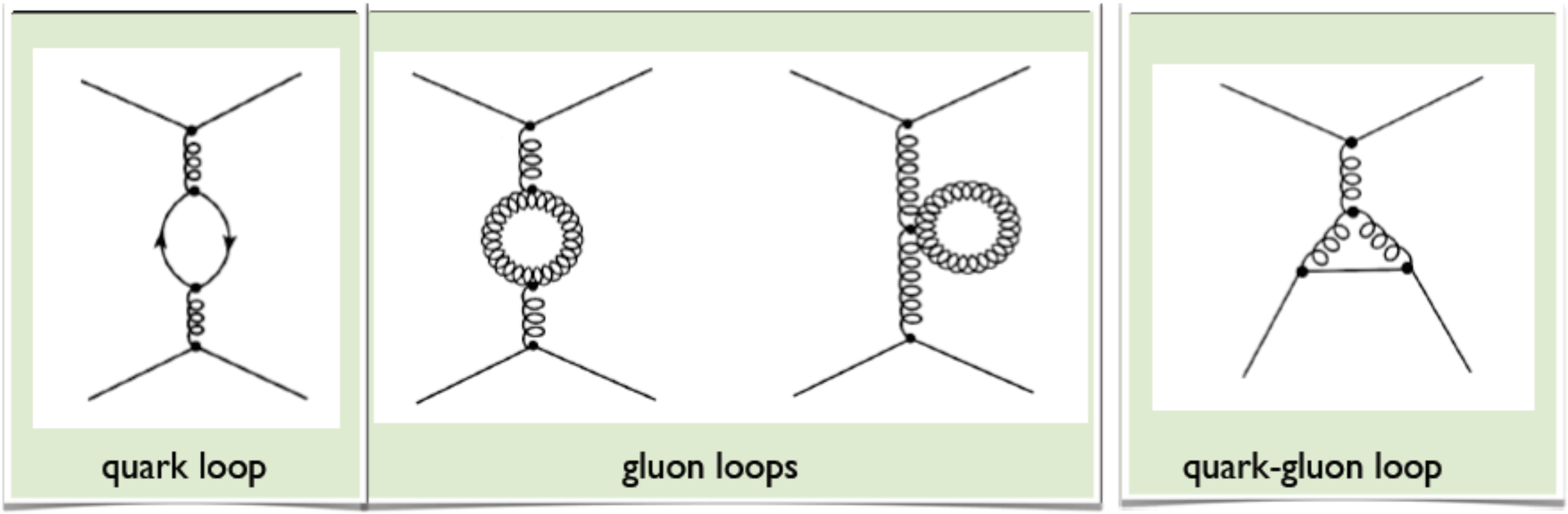

Quark loops: increase $\alpha_s(|q^2|)$ with $|q^2|$

Gluon loops: decrease $\alpha_s(|q^2|)$ with $|q^2|$

$$\alpha_s(|q^2|) = \frac{\alpha_s(\mu^2)}{1 + [\alpha_s(\mu^2)/12\pi](11n - 2f)\ln(|q^2|/\mu^2)} \quad (|q^2| \gg \mu^2)$$

n: # of colors(=3)
f : # of flavors, which are open at $|q^2|$

Leading log approximation. This formula gives the running of $\alpha_s(|q^2|)$. If we know it at $|q^2|=\mu$, we can calculate in for every $|q^2|$.

Running of α_s:

$$\alpha_s(|q^2|) = \frac{\alpha_s(\mu^2)}{1 + [\alpha_s(\mu^2)/12\pi](11n - 2f)\ln(|q^2|/\mu^2)} \quad (|q^2| \gg \mu^2)$$

The energy scale μ must be chosen such that $\alpha_s(|q^2|) < 1$, otherwise the power expansion does not converge and perturbation theory is not valid.

One can define the Λ - Parameter:

$$\ln \Lambda^2 = \ln \mu^2 - 12\pi/[(11n - 2f)\alpha_s(\mu^2)]$$

Then the single parameter Λ determines the running of α

$$\alpha_s(|q^2|) = \frac{12\pi}{(11n - 2f)\ln(|q^2|/\Lambda^2)} \quad (|q^2| \gg \Lambda^2)$$

From experimental measurements on finds: 100 MeV < Λ < 350 MeV

One usually choses $\mu = m_Z$ as a reference scale, since $\alpha_s(m_z^2)$ has been measured very precisely at LEP. With the formula above, values measured at other energies can be extrapolated to m_Z.

Running of α_s:

The renormalization scale dependence of the effective QCD coupling $\alpha_s = g_s^2/4\pi$ is controlled by the β-function:

$$\mu \frac{\partial \alpha_s}{\partial \mu} = 2\beta(\alpha_s) = -\frac{\beta_0}{2\pi}\alpha_s^2 - \frac{\beta_1}{4\pi^2}\alpha_s^3 - \frac{\beta_2}{64\pi^3}\alpha_s^4 - \cdots ,$$

$$\beta_0 = 11 - \frac{2}{3} n_f ,$$

$$\beta_1 = 51 - \frac{19}{3} n_f ,$$

$$\beta_2 = 2857 - \frac{5033}{9} n_f + \frac{325}{27} n_f^2 ,$$

If one solves the differential equation an integration constant appears, which is the value of αs at a fixed reference scale μ_0. One often chooses $\mu_0 = M_Z$ as mentioned earlier.

The value of $\alpha s(\mu)$ can then be calculated from: $\log(\mu^2/\mu_0^2) = \int_{\alpha_s(\mu_0)}^{\alpha_s(\mu)} \frac{d\alpha}{\beta(\alpha)}$

Experimental measurements of α_s:

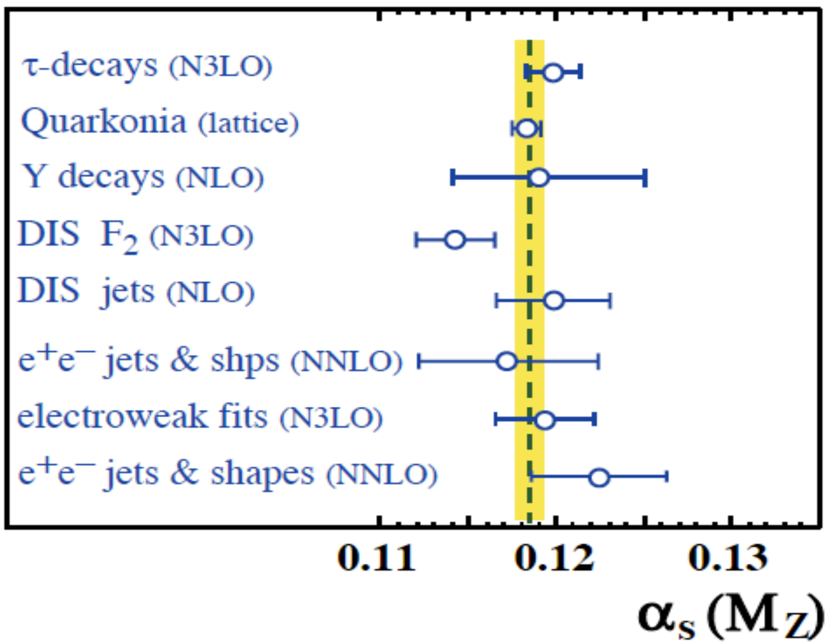

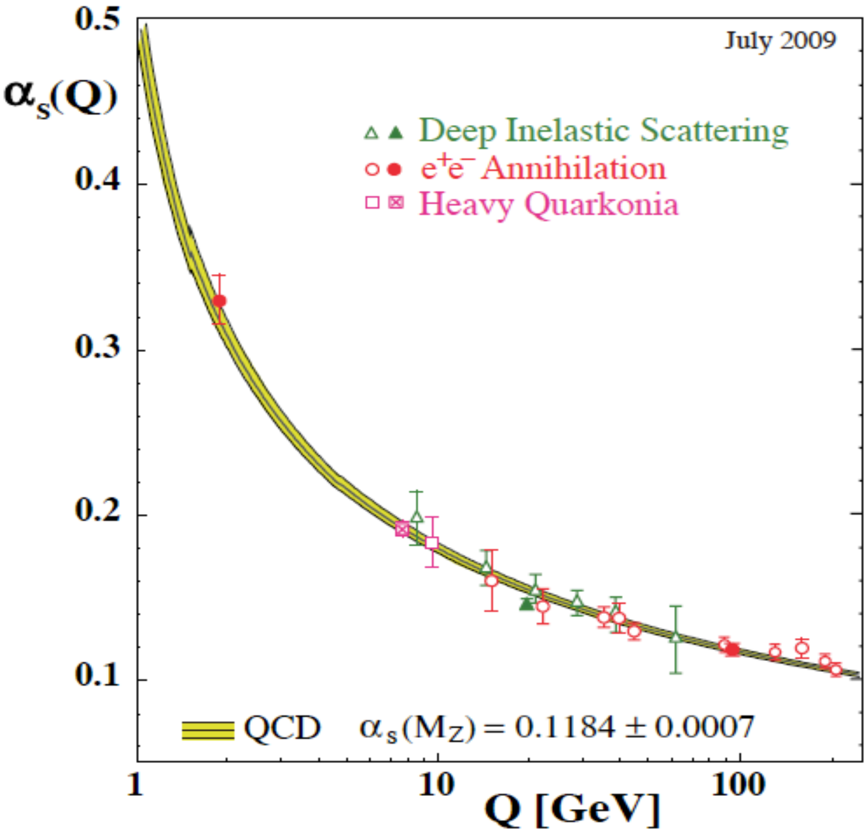

Summary of measurements of α_s (m_Z^2), used as input for the world average value (from Particle Data Group).

Summary of measurements of α_s as a function of the respective energy scale Q (from Particle Data Group).

5.3 Jet production at hadron colliders

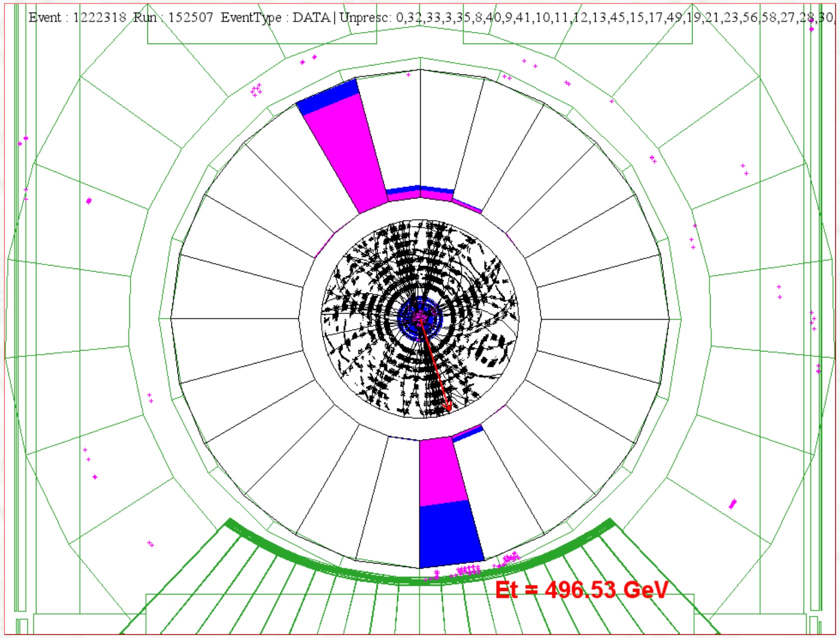

CDF (ϕ-r view)

Dijet mass = 1364 GeV/c^2

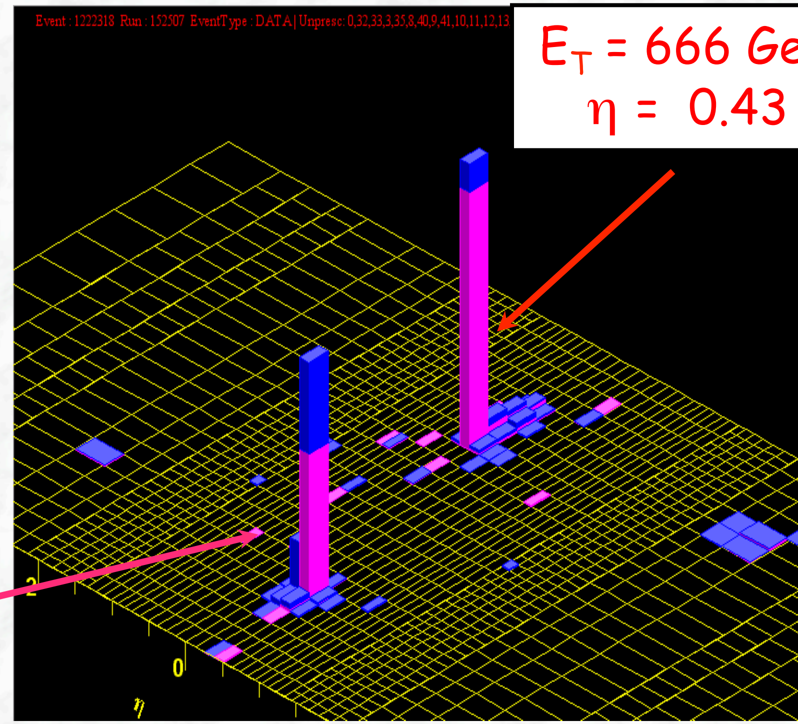

E_T = 666 GeV
η = 0.43

E_T = 633 GeV
η = -0.19

A two jet event at the Tevatron (CDF)

5.3.1 Theoretical calculations

Leading order

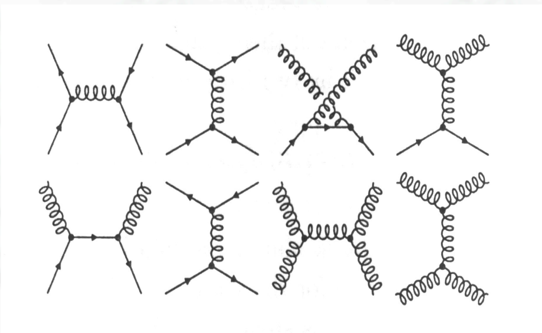

…some NLO contributions

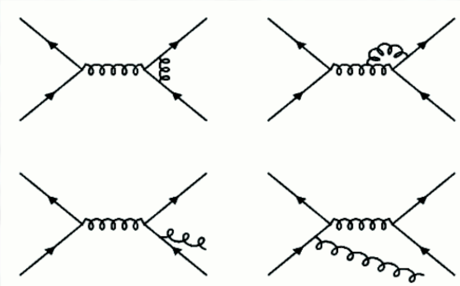

$$\frac{d\hat{\sigma}}{d\hat{t}}(ab \to cd) = \frac{|M|^2}{(16\pi\hat{s}^2)}$$

Subprocess	$\lvert\mathcal{M}\rvert^2/g_s^4$	$\lvert\mathcal{M}(90°)\rvert^2/g_s^4$
$qq' \to qq'$, $q\bar{q}' \to q\bar{q}'$	$\frac{4}{9}\frac{\hat{s}^2+\hat{u}^2}{\hat{t}^2}$	2.2
$qq \to qq$	$\frac{4}{9}\left(\frac{\hat{s}^2+\hat{u}^2}{\hat{t}^2}+\frac{\hat{s}^2+\hat{t}^2}{\hat{u}^2}\right)-\frac{8}{27}\frac{\hat{s}^2}{\hat{u}\hat{t}}$	3.3
$q\bar{q} \to q'\bar{q}'$	$\frac{4}{9}\frac{\hat{t}^2+\hat{u}^2}{\hat{s}^2}$	0.2
$q\bar{q} \to q\bar{q}$	$\frac{4}{9}\left(\frac{\hat{s}^2+\hat{u}^2}{\hat{t}^2}+\frac{\hat{t}^2+\hat{u}^2}{\hat{s}^2}\right)-\frac{8}{27}\frac{\hat{u}^2}{\hat{s}\hat{t}}$	2.6
$q\bar{q} \to gg$	$\frac{32}{27}\frac{\hat{u}^2+\hat{t}^2}{\hat{u}\hat{t}}-\frac{8}{3}\frac{\hat{u}^2+\hat{t}^2}{\hat{s}^2}$	1.0
$gg \to q\bar{q}$	$\frac{1}{6}\frac{\hat{u}^2+\hat{t}^2}{\hat{u}\hat{t}}-\frac{3}{8}\frac{\hat{u}^2+\hat{t}^2}{\hat{s}^2}$	0.1
$qg \to qg$	$\frac{\hat{s}^2+\hat{u}^2}{\hat{t}^2}-\frac{4}{9}\frac{\hat{s}^2+\hat{u}^2}{\hat{u}\hat{s}}$	6.1
$gg \to gg$	$\frac{9}{4}\left(\frac{\hat{s}^2+\hat{u}^2}{\hat{t}^2}+\frac{\hat{s}^2+\hat{t}^2}{\hat{u}^2}+\frac{\hat{u}^2+\hat{t}^2}{\hat{s}^2}+3\right)$	30.4

- Right: Results of the LO matrix elements for the various scattering processes, expressed in terms of the Mandelstam variables s, t and u. (Kripfganz et al, 1974);
- gg scattering is the dominant contribution under $\eta = 0$;
  (sensitivity to gluons, sensitivity to gluon self-coupling, as predicted by QCD)
- NLO predictions have meanwhile been calculated (2002).

The composition of the partons involved as function of the p_T of the jet at the Tevatron:

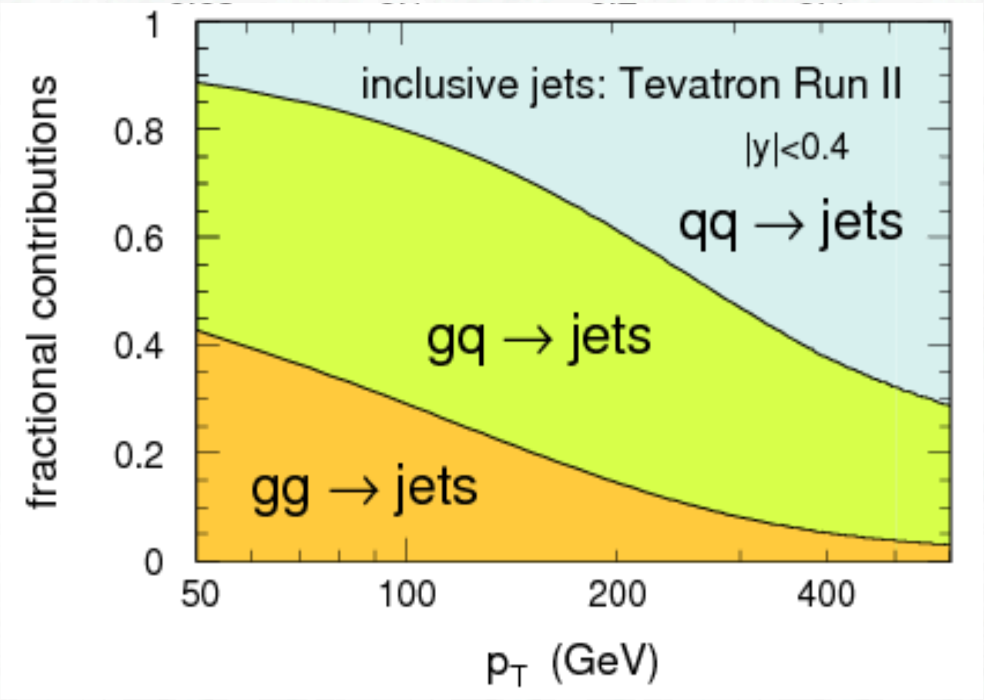

Tevatron,
ppbar, $\sqrt{s}$ = 1.96 TeV,
central region $|\eta| < 0.4$

- qq scattering dominates at high p_T
- However, gluons contribute over the full range

5.3.2 Experimental issues

$$d^2\sigma / dp_T\, d\eta \;=\; N \;/\; (\varepsilon \cdot L \cdot \Delta p_T \cdot \Delta\eta)$$

- In principle a simple counting experiment

- However, steeply falling p_T spectra are sensitive to jet energy scale uncertainties and resolution effects (migration between bins) → corrections (unfolding) to be applied

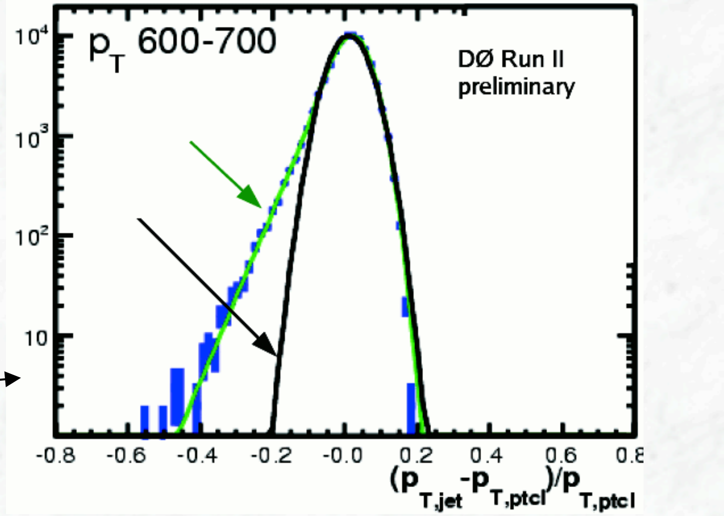

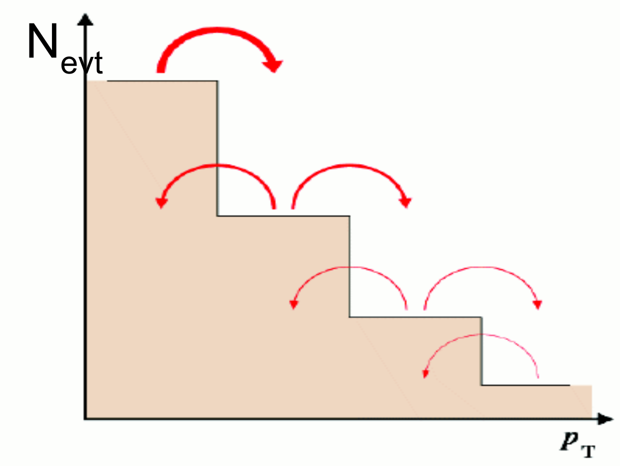

- Sensitivity to jet energy scale uncertainty:
  DØ: 1% energy scale error
  → 10% cross section uncert. at $|\eta|<0.4$

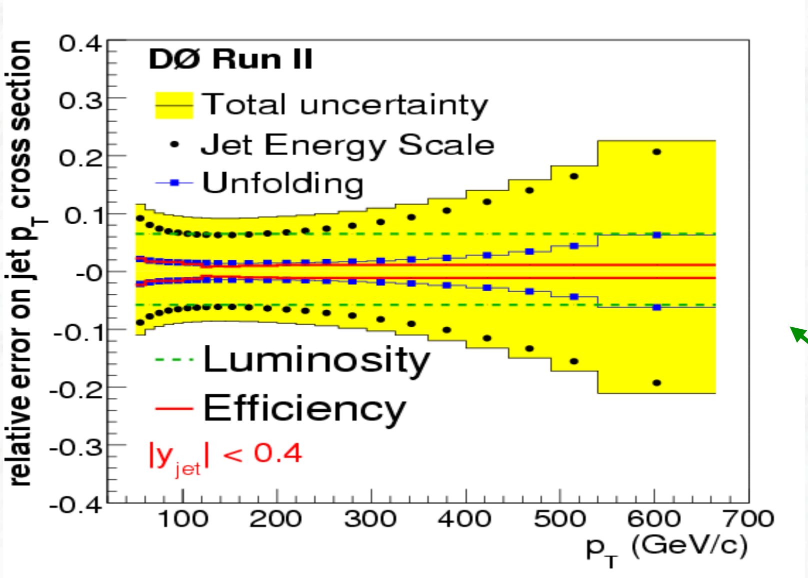

Major exp. errors:
energy scale, luminosity (6%),…

Jet reconstruction and energy measurement

- A jet is NOT a well defined object
  (fragmentation, gluon radiation, detector response)

- The detector response is different for particles interacting electromagnetically (e,γ) and for hadrons
  → for comparisons with theory, one needs to correct back the calorimeter energies to the „particle level" (particle jet)
  Common ground between theory and experiment

- One needs an algorithm to define a jet and to measure its energy
  conflicting requirements between experiment and theory (exp. simple, e.g. cone algorithm, vs. theoretically sound (no infrared divergencies))

- Energy corrections for losses of fragmentation products outside jet definition and underlying event or pileup energy inside

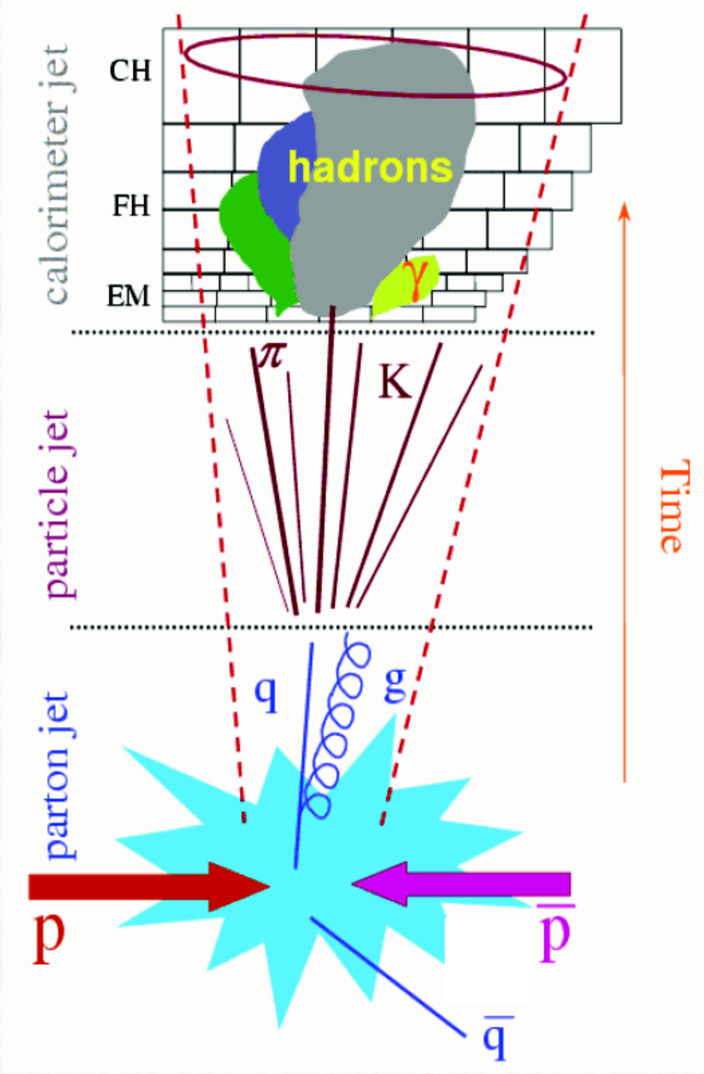

Infrared and collinear safetiness

- To compare an experimental result with theory, often jet counting is involved (for example, inclusive jet cross section
- Need to have a jet reconstruction algorithm which is "collinear" and "infrared" safe

- Collinear safe: jet definition independent on the presence of partons radiated collinear to the quark

- Infrared safe: jet definition independent on the presence of soft radiation

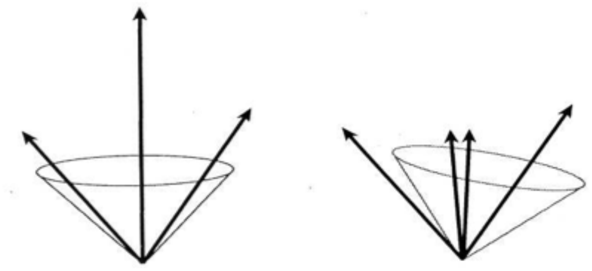

Figure 4.3: *Collinear safety violation. The splitting of one tower into two can change the jet properties.*

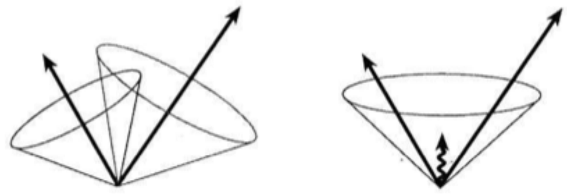

Figure 4.2: *Infrared safety violation: the radiation of a soft gluon can change the jet properties.*

A family of "safe" algorithms

- The k_T family algorithms are the most used nowadays
- For every pair of particle I,j compute d_{ij}

$$d_{ij} = min(E^a_{Ti}, E^a_{Tj})\frac{\Delta\eta^2 + \Delta\phi^2}{R^2}$$ i != j

$$d_{ij} = E_T^2$$ i = j

- If a = -1, one has the Anti-k_t algorithm

Find $d_{min} = \min(d_i, d_{ij})$.

If $d_{min} = d_{ij}$ for some j, merge tower i and j to a new tower k with momentum $p_k^\mu = p_j^\mu + p_j^\mu$.

If $d_{min} = d_i$ then a jet is found.

Iterate until the list of tower is empty.

Main corrections:

- In general, calorimeters show different response to electrons/photons and hadrons
- Subtraction of offset energy not originating from the hard scattering (inside the same collision or pile-up contributions, use minimum bias data to extract this)
- Correction for jet energy out of cone (corrected with jet data + Monte Carlo simulations)

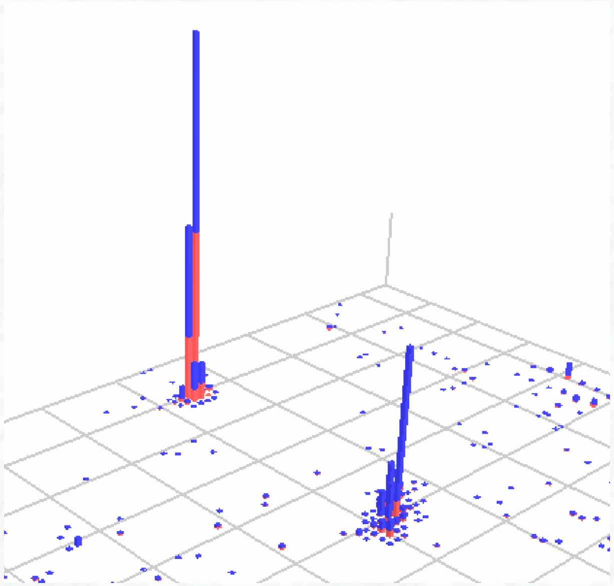

Jet Energy Scale

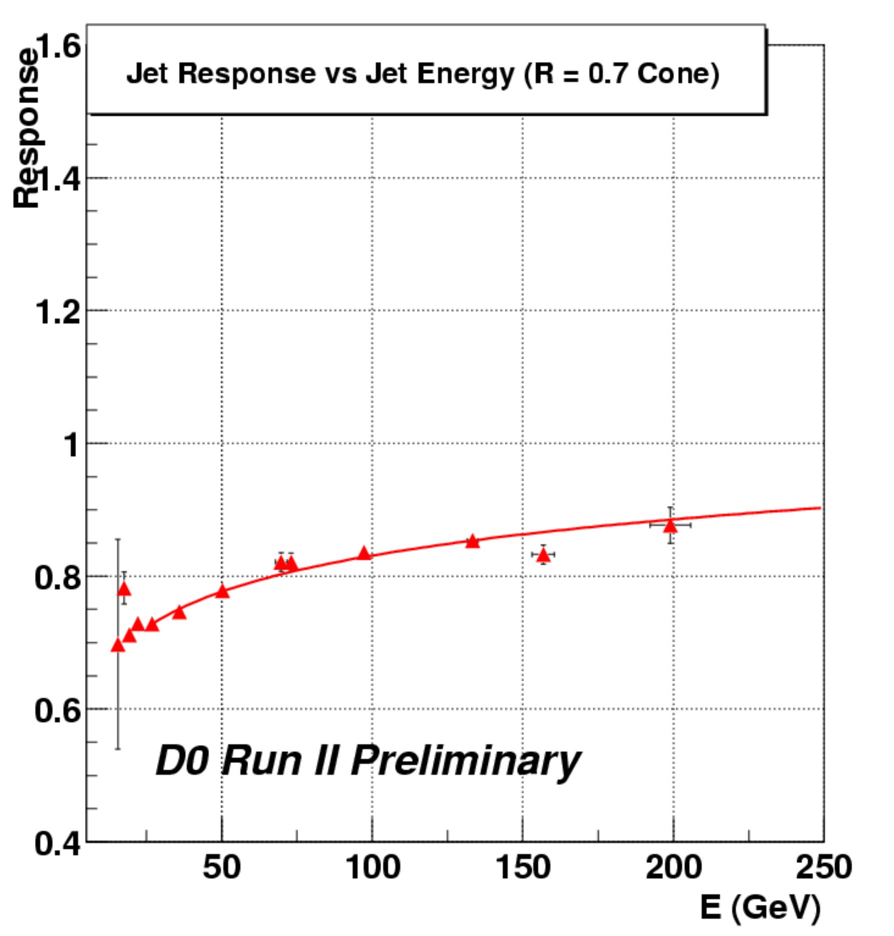

Jet response correction in DØ:

- Measure response of particles making up the jet

- Use photon + jet data - calibrate jets against the better calibrated photon energy

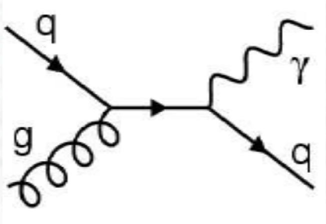

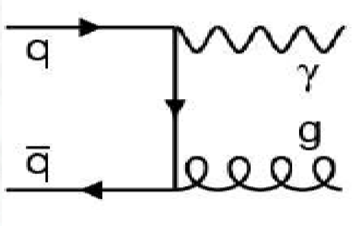

- Achieved jet energy scale uncertainty:

  DØ: $\Delta E / E$ ~1-2%
  (excellent result, a huge effort)

Jet energy scale at the LHC

- A good jet-energy scale determination is essential for many QCD measurements
  (arguments similar to Tevatron, but kinematic range (jet p_T) is larger, ~20 GeV – ~3 TeV)

- Propagate knowledge of the em scale to the hadronic scale, but several processes are needed to cover the large p_T range

Measurement process	Jet p_T range
Z + jet balance	$20 < p_T < 100 - 200$ GeV
γ + jet balance	$50 < p_T < 500$ GeV (trigger, QCD background)
Multijet balance	$500 \text{ GeV} < p_T$

Reasonable goal: 5-10% in first runs (1 fb^{-1})
1- 2% long term

Example: Z + jet balance

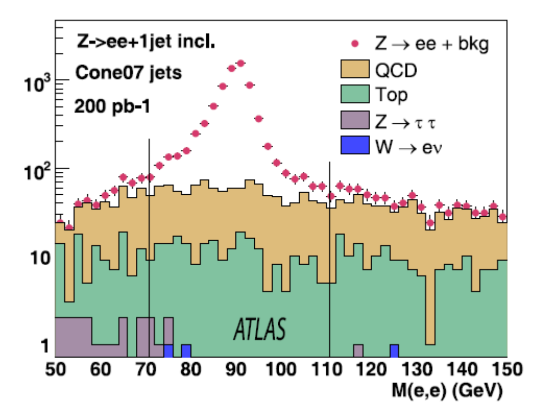

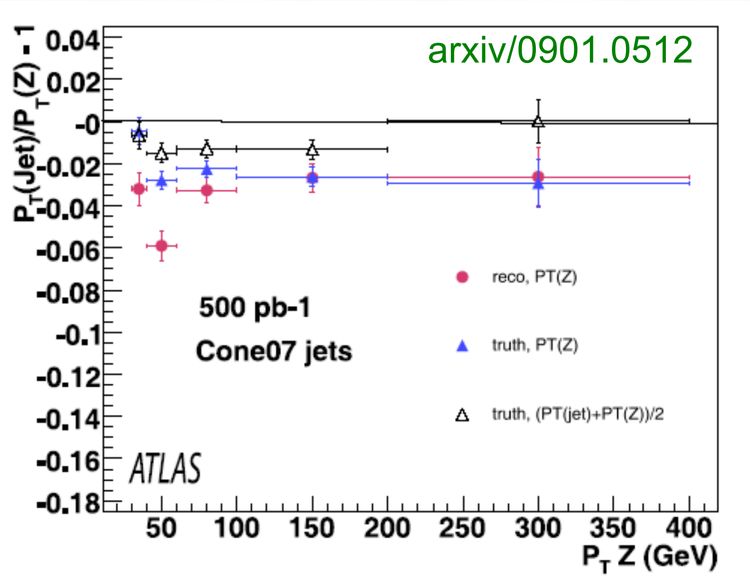

Stat. precision (500 pb^{-1}): 0.8%
Systematics: 5-10% at low p_T, 1% at high p_T

Test of QCD Jet production

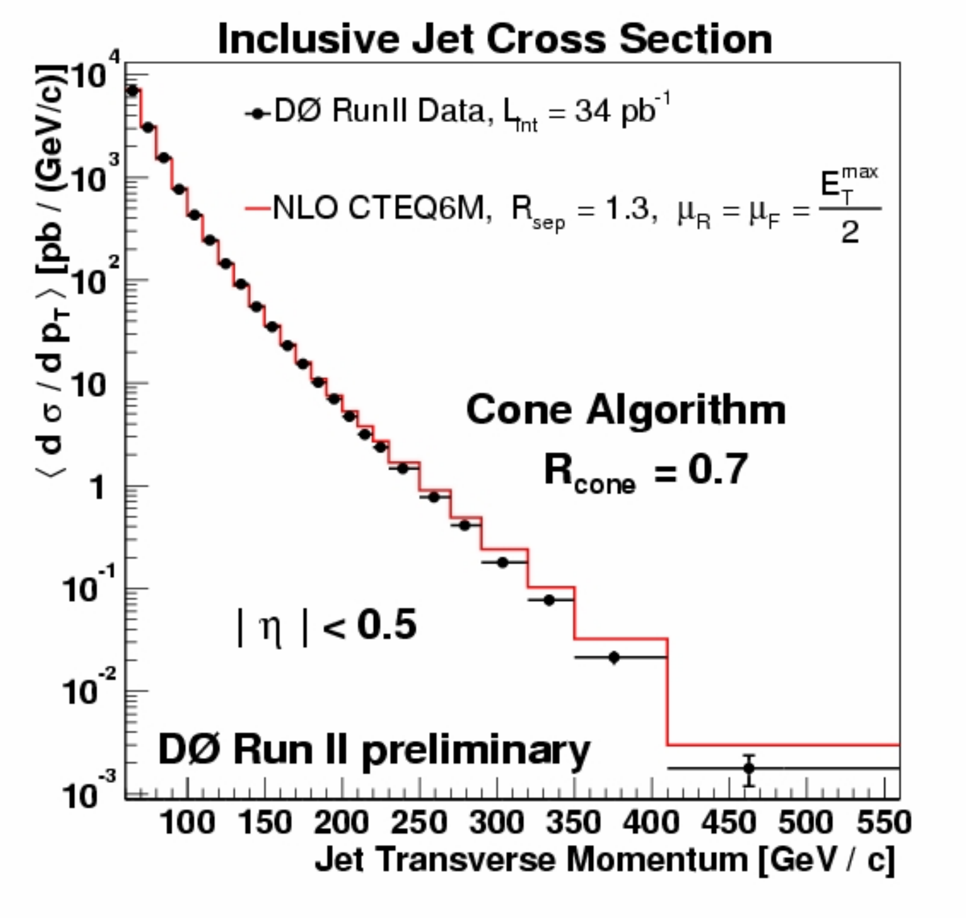

An **"early"** result from the DØ experiment (34 pb^{-1})

Inclusive Jet spectrum as a function of Jet-P_T

very good agreement with NLO pQCD calculations over many orders of magnitude !

within the large theoretical and experimental uncertainties

Double differential distributions in p_T and η

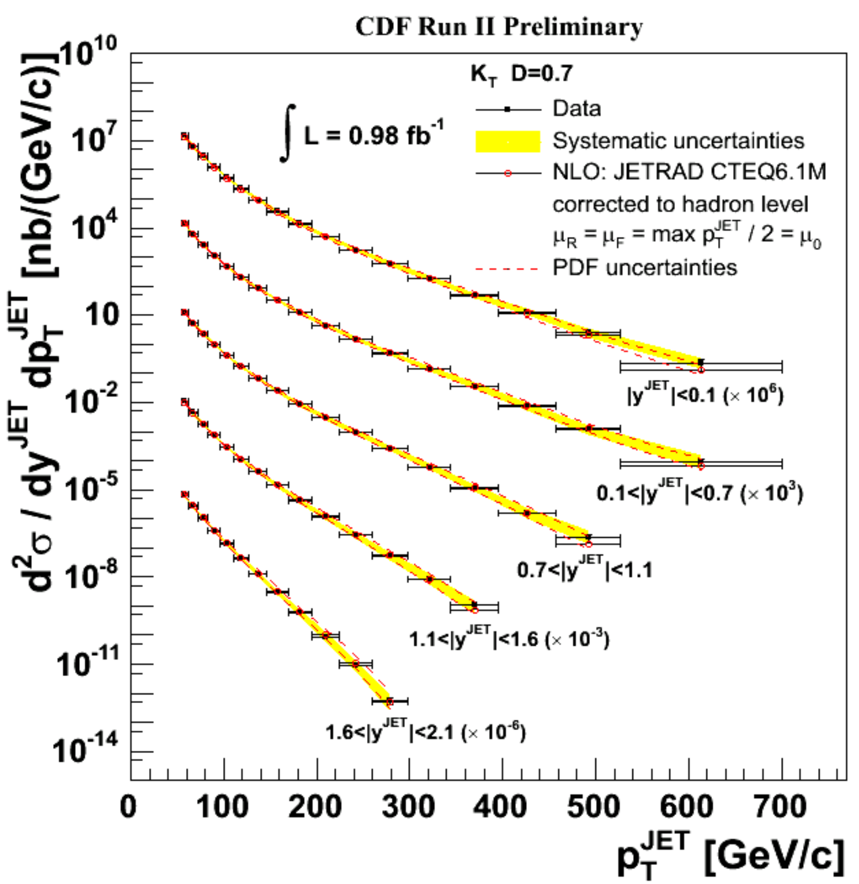

PRD 78 052006 ('08)

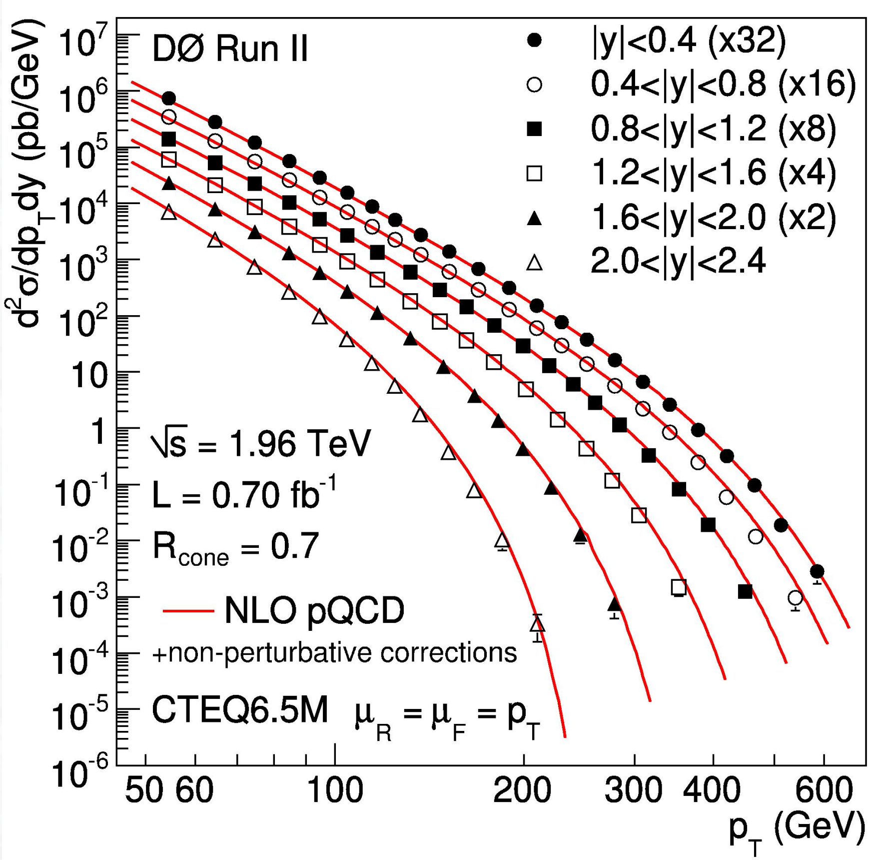

PRL 101 062001 ('08)

- Measurement in 5-6 different rapidity bins, over 9 orders of magnitude, up to p_T ~650 GeV
- Data corresponding to ~ 1 fb^{-1} (CDF) and 0.7 fb^{-1} (DØ)

Comparison between data and theory

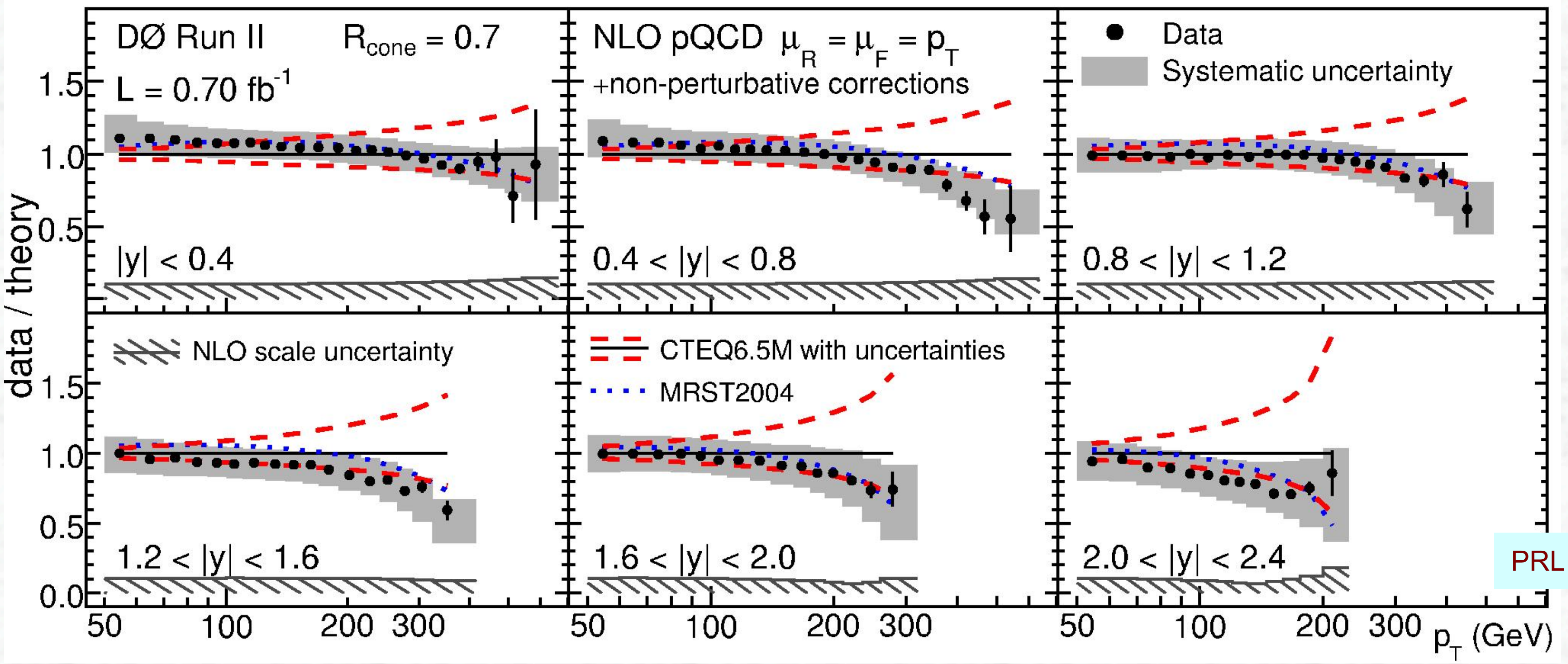

PRL 101 062001 ('08)

- **CDF and DØ agree within uncertainties**

- Experimental uncertainties are smaller than the pdf uncertainties
  (in particular large for large x, gluon distribution)

- Wait for updated (2009) parametrizations
  (plans to include Tevatron data, to better constrain the high x-region)

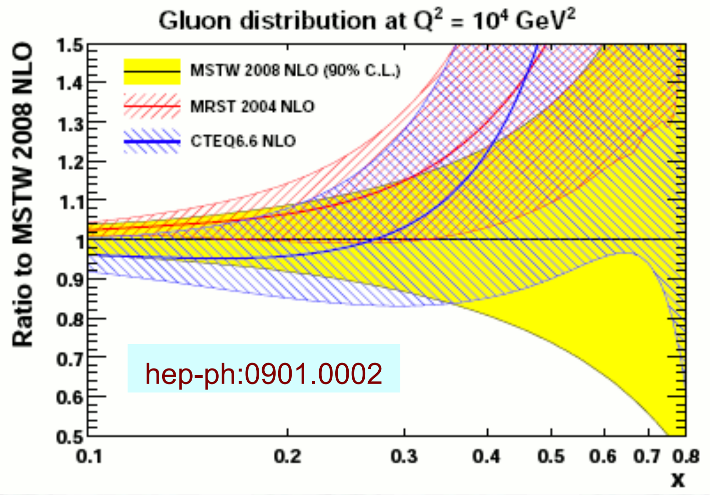

hep-ph:0901.0002

Di-jet angular distributions

- *reduced sensitivity to Jet energy scale*
- *sensitivity to higher order QCD corrections preserved*

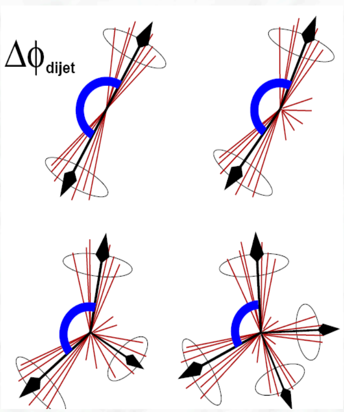

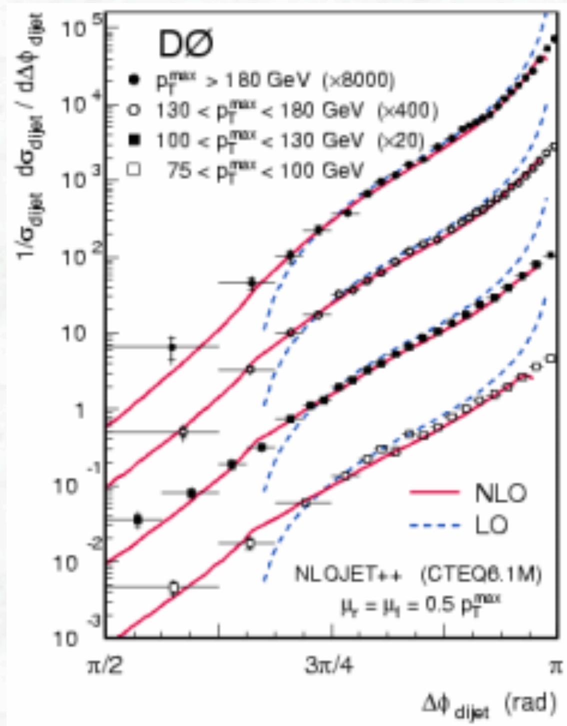

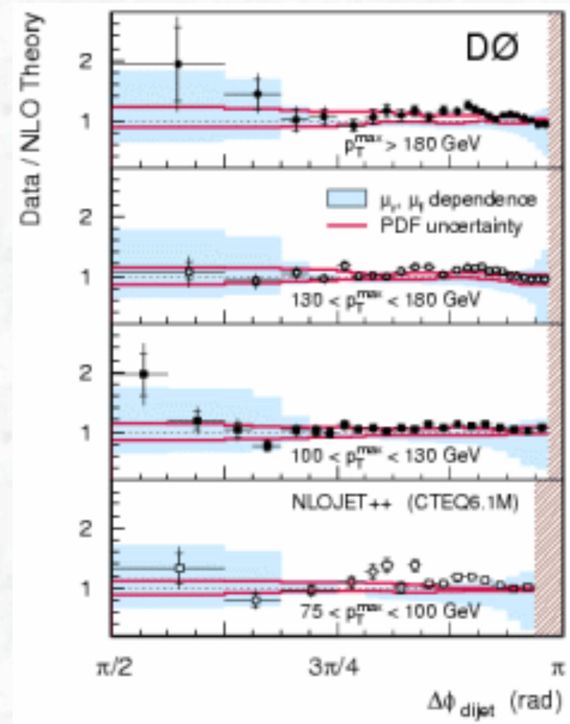

Good agreement with
next-to-leading order QCD predictions

High p_T jet events at the LHC

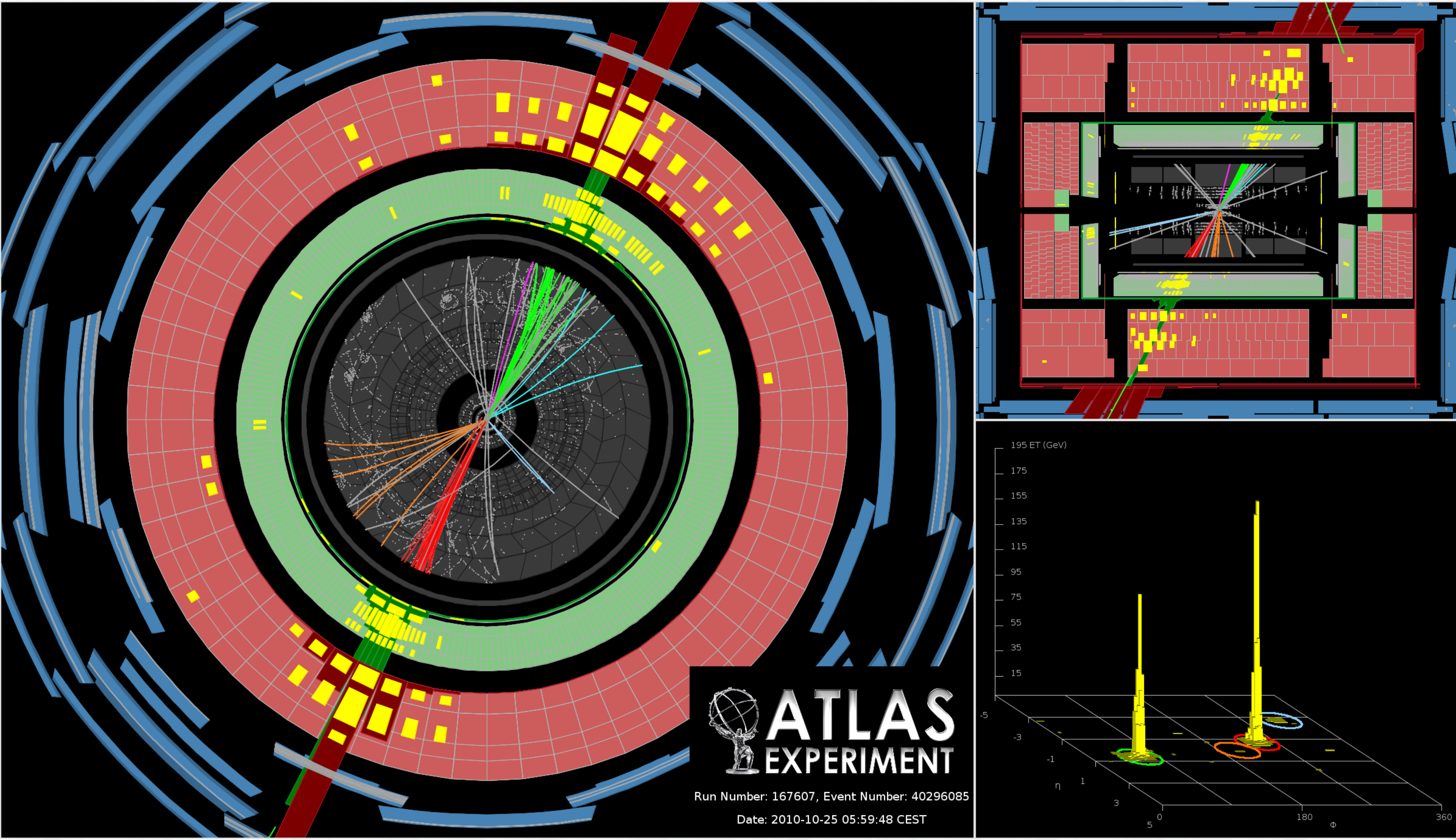

Event display that shows the highest-mass central dijet event collected during 2010, where the two leading jets have an invariant mass of 3.1 TeV. The two leading jets have (p_T, y) of (1.3 TeV, -0.68) and (1.2 TeV, 0.64), respectively. The missing E_T in the event is 46 GeV. From ATLAS-CONF-2011-047.

An event with a high jet multiplicity at the LHC

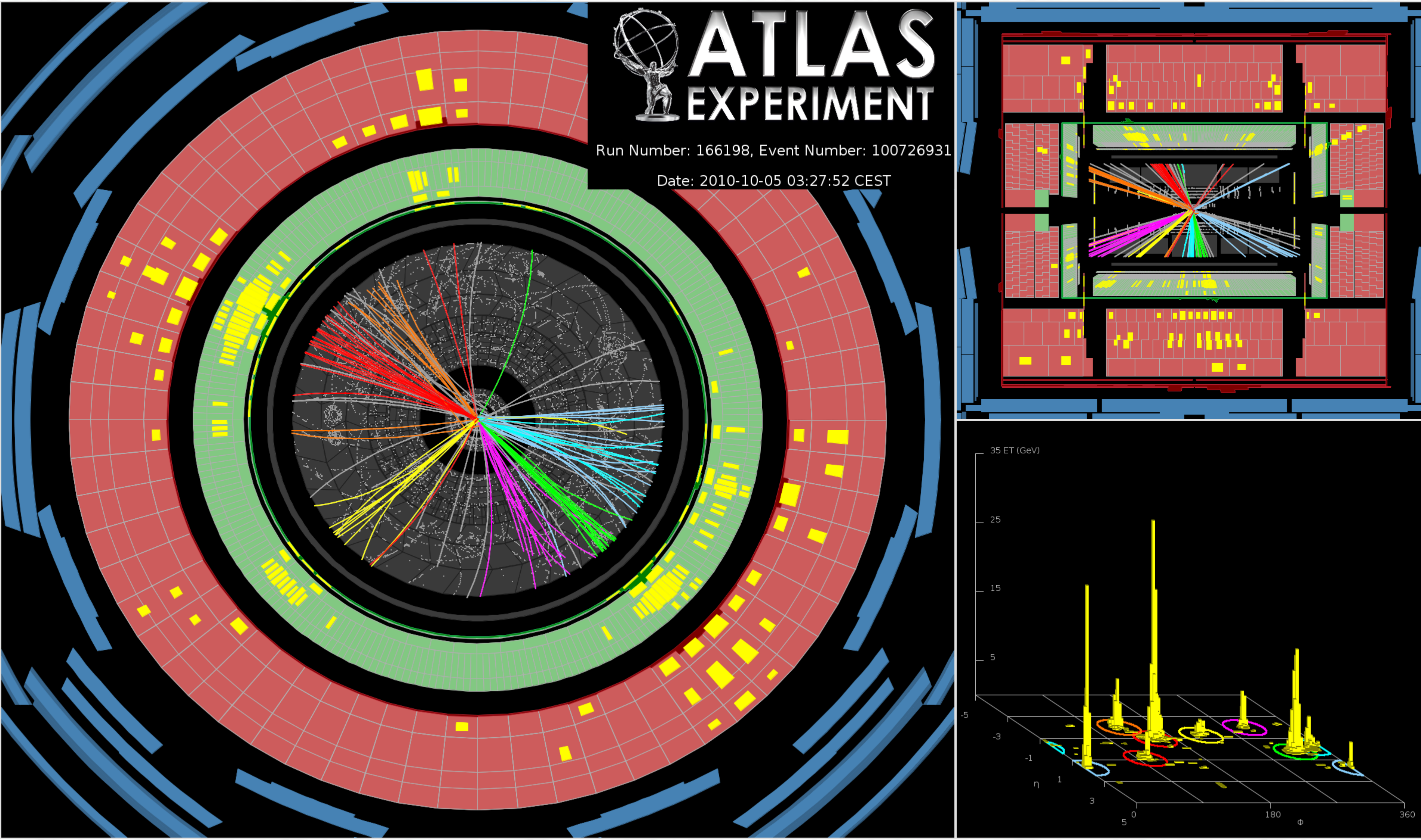

The highest jet multiplicity event collected by the end of October 2010, counting jets with p_T greater than 60 GeV: this event has eight. 1st jet (ordered by p_T): p_T = 290 GeV, η = -0.9, φ = 2.7; 2nd jet: p_T = 220 GeV, η = 0.3, φ = -0.7 Missing E_T = 21 GeV, φ = -1.9, Sum E_T = 890 GeV. The event was collected on 5 October 2010.

Initial jet energy scale calibration:

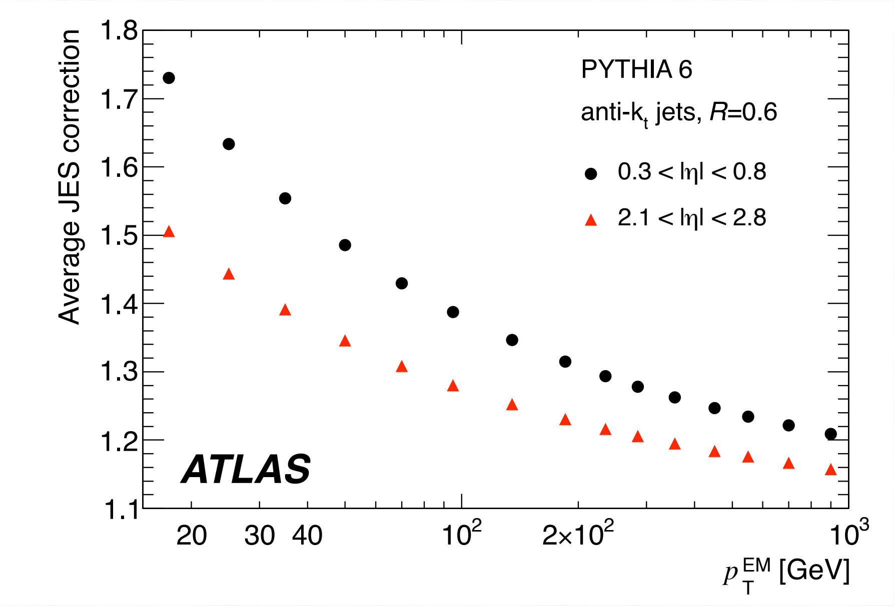

Average jet energy scale correction, evaluated using PYTHIA 6, as a function of jet transverse momentum at the EM scale for jets in the central barrel (black circles) and endcap (red triangles) regions, shown in EM scale p_T bins and η regions.

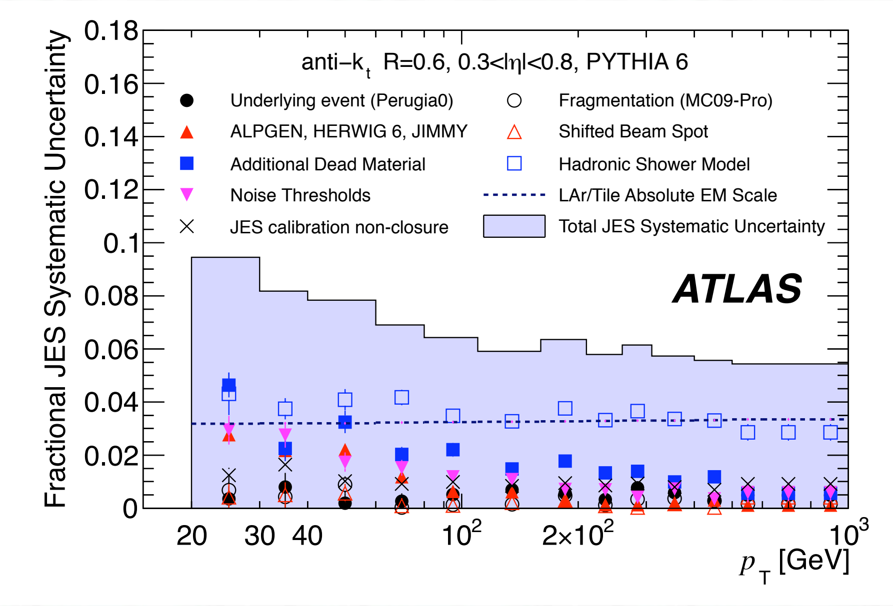

Fractional jet energy scale systematic uncertainty as a function of p_T for jets in the pseudorapidity region $0.3 < |\eta| < 0.8$ in the barrel calorimeter. The total systematic uncertainty is shown as the solid light blue area. The individual sources are also shown, with statistical errors if applicable.

Further improvements

Several in-situ techniques have reduces the jet energy scale uncertainty significantly:

- Single particle response
- Di-jet balance

And, more recently:

- Gamma + jet balance
- Z + jet balance

Strong impact on all measurements involving jets